



Transit Time index (TTi) as an adaptation of the humification index to illustrate transit time differences in karst hydrosystems: application to the karst springs of the Fontaine de Vaucluse system (southeastern France)

Leïla Serène, Christelle Batiot-Guilhe, Naomi Mazzilli, Christophe Emblanch, Milanka Babic, Julien Dupont, Roland Simler, Matthieu Blanc, Gérard Massonnat

► To cite this version:

Leïla Serène, Christelle Batiot-Guilhe, Naomi Mazzilli, Christophe Emblanch, Milanka Babic, et al.. Transit Time index (TTi) as an adaptation of the humification index to illustrate transit time differences in karst hydrosystems: application to the karst springs of the Fontaine de Vaucluse system (southeastern France). *Hydrology and Earth System Sciences*, 2022, 26 (19), pp.5035-5049. 10.5194/hess-26-5035-2022 . hal-03842488

HAL Id: hal-03842488

<https://hal.science/hal-03842488>

Submitted on 7 Nov 2022

HAL is a multi-disciplinary open access archive for the deposit and dissemination of scientific research documents, whether they are published or not. The documents may come from teaching and research institutions in France or abroad, or from public or private research centers.

L'archive ouverte pluridisciplinaire **HAL**, est destinée au dépôt et à la diffusion de documents scientifiques de niveau recherche, publiés ou non, émanant des établissements d'enseignement et de recherche français ou étrangers, des laboratoires publics ou privés.



Distributed under a Creative Commons Attribution 4.0 International License



Transit Time index (TTi) as an adaptation of the humification index to illustrate transit time differences in karst hydrosystems: application to the karst springs of the Fontaine de Vaucluse system (southeastern France)

Leïla Serène¹, Christelle Batiot-Guilhe¹, Naomi Mazzilli², Christophe Emblanch², Milanka Babic², Julien Dupont², Roland Simler², Matthieu Blanc³, and Gérard Massonnat⁴

¹HSM, Univ. Montpellier, CNRS, IMT, IRD, Montpellier, France

²UMR 1114 EMMAH (AU-INRAE), Université d'Avignon, 84000 Avignon, France

³Independent Researcher, Montpellier, France

⁴Total Energies, CSTJF, Avenue Larribau, CEDEX 64018 Pau, France

Correspondence: Leïla Serène (leila.serene@umontpellier.fr)

Received: 9 March 2022 – Discussion started: 31 March 2022

Revised: 6 June 2022 – Accepted: 19 June 2022 – Published: 11 October 2022

Abstract. Transit time can be estimated thanks to natural tracers, but few of them are usable in the 0–6-month range. The main purpose of this work is to analyze the potential of the ratio of heavy- to light-weight organic compounds (the humification index (HIX); Ohno, 2002; Zsolnay et al., 1999) as a natural tracer of short transit time (Blondel et al., 2012). Critical analysis of former studies shows that although the link between HIX and transit time seems consistent, the whole methodological approach needs to be consolidated. Natural organic matter fluorescence from 289 groundwater samples from four springs and 10 flow points located in the unsaturated zone of the Vaucluse karst system is characterized by parallel factor analysis (PARAFAC) thanks to the excitation–emission matrix (EEM), thus (i) allowing for the identification of main fluorescent compounds of sampled groundwater and (ii) evidencing the inadequacy of HIX 2D emission windows to characterize groundwater organic matter. We then propose a new humification index called the Transit Time index (TTi) based on the Ohno (2002) formula but using PARAFAC components of heavy and light organic matter from our samples instead of 2D windows. Finally, we evaluate TTi relevance as a transit time tracer by (i) performing a detailed analysis of its dynamics on a selected spring (Millet) and (ii) comparing its mean value over karst springs of the Vaucluse karst system. Principal component analysis (PCA) of TTi and other hydrochemical parameters monitored

at Millet spring put in relief the different ranges of transit time associated with the different organic matter compounds. PCA results also provide evidence that TTi can detect a small proportion of fast infiltration water within a mix, while other natural tracers of transit time provide no or less sensitive information. TTi distributions at monitored karst springs are consistent with relative transit times expected for the small-scale, short average transit time systems. TTi thus appears as a relevant qualitative tracer of transit time in the 0–6-month range where existing tracers fail and may remain applicable, even in the case of anthropic contamination thanks to PARAFAC modeling. Transforming it into quantitative information is a challenging task which may be possible thanks to intensive studies of organic matter degradation kinetics in natural waters with the help of radiogenic isotope usage or an artificial tracer test.

1 Introduction

Karst aquifers are essential for water supply at both global and local scales as they provide 9.2 % of the world's drinking water and contribute to 13 % of the total global withdrawal of groundwater (Stevanović, 2019). But karsts are also really complex and compartmentalized systems which offer very different paths to the infiltrated water. The hier-

archized network of karst conduits allows for a fast transit of recharge which is very specific to karst systems (White, 2002) and makes it essential to develop natural tracers of transit on short timescales (< 6 months). Natural tracers of stored water include major element contents, isotopes, and dissolved gas (Malík et al., 2016; Musgrove et al., 2019; Pérotin et al., 2021; Zhang et al., 2021), but few of these tracers allow fast infiltration to be characterized. Indeed, natural tracers of transit time of this range must, by definition, see their contents vary at this timescale. While variations in inorganic compounds are small on this timescale, living and organic components of water like bacteria, total organic carbon (TOC), or natural organic matter fluorescence (Batiot et al., 2003; Lapworth et al., 2008; Mudarra et al., 2011; Pronk et al., 2009; Sorensen et al., 2020) are suited to this goal. Indeed, TOC represents the quantity of organic matter present in the water, and its mineralization (or degradation) is complete after 6 months (Batiot, 2002). Fluorescent organic matter is a small part of the total organic matter represented by TOC and will therefore also be completely degraded after a maximum of 6 months. Its potential as a natural tracer of groundwater was already put in relief in Baker and Lamont-Black (2001). Our study focuses on fluorescent organic matter and its relation with transit time through the humification index (HIX), as initially proposed by Blondel et al. (2012).

Fluorescent organic matter compounds are degraded in the natural environment. The rate of this degradability is constrained by two aspects: the type of organic matter and biological activity. The influence of the organic matter type is well documented; complicated molecules of organic matter have a higher emission wavelength and less digestibility (Zsolnay, 1999). For example, humic-like organic matter is less digestible than protein-like organic matter and thus takes more time to be degraded.

The humification index (HIX) expresses the maturation level of organic matter. Humification refers to the gradual transition of organic matter to highly metabolized compounds (humins). HIX is defined as the ratio of humic to non-humic compounds. Because this ratio is related to the maturation of organic matter, it has the potential to be related to transit times in the range 0 to 6 months (before maturation is complete).

In a study which aimed at identifying dissolved organic matter (DOM) sources in soil and sediment waters, Zsolnay (1999) proposed a methodology to derive HIX from fluorescence measurements. He identified the excitation wavelength most representative of fluorescent organic matter in soil water (254 nm). Next, he identified emissions wavelengths corresponding to light (L from 300 to 345 nm) and heavy (H from 435 to 480 nm) organic compounds in the emission spectra with the assumption that emission wavelengths of fluorescent molecules increase while molecules get more condensed (Ewald et al., 1988; Zsolnay et al., 1999). HIX was then defined by the ratio H/L of the integral under the emission curve of 2D spectra at 254 nm of excitation wavelength.

This way of calculating HIX is dependent on DOM concentration because of the inner-filtering effect (Ohno, 2002). The inner-filtering effect results from either the absorption of excitation light by fluorescent molecules before it gets to the monitored zone (primary inner-filtering effect) or the absorption of emission light coming from photons (secondary inner-filtering effect; Tucker et al., 1992). Using the H/L ratio to calculate HIX permits correction for the primary inner-filtering effect which affects each wavelength equally. But the secondary inner-filtering effect still needs to be corrected if different study sites are to be compared (Mobed et al., 1996). Ohno (2002) thus proposed another HIX formula that corrects for both inner-filter effects:

$$\text{HIX} = \frac{H}{L + H}. \quad (1)$$

A quantitative relation between HIX and transit time was proposed by Blondel et al. (2012) based on natural fluorescence monitoring of four flow points collected in the unsaturated zone of the Fontaine de Vaucluse system (France) during two hydrological cycles (2006–2007 and 2007–2008). Careful examination of this work revealed several methodological weaknesses. The calculated HIX used Zsolnay's formula (Zsolnay, 1999), which lacks secondary inner-filtering effect correction and thus prevents comparison between study sites or flows. The excitation wavelength was 260 nm instead of 254 nm as recommended by Zsolnay (1999). In any case, Zsolnay emission windows were calibrated for soil water; it is thus possible that they may be unsuitable for groundwater. The relation between HIX and transit time was obtained by considering the mean total organic carbon (TOC) value for each hydrological cycle and each flow point: the relation between transit time and TOC proposed by Batiot et al. (2003) allowed transit time values to be connected to HIX. However, this relation was based on a very limited number of samples and had a high uncertainty.

In spite of these limitations, Blondel's study results were consistent and led to the identification of a clear link between HIX and transit time. Based on the critical analysis of these previous studies, we first analyzed water fluorescence on 289 groundwater samples from four springs and 10 flow points located in the unsaturated zone of the Vaucluse karst system. The 2D spectra of organic matter fluorescence were compared with Zsolnay emission windows. Main organic matter fluorescent compounds in water samples were identified based on parallel factor analysis (PARAFAC) and bibliographical review. We then proposed a new humification index called the Transit Time index (TTi) based on the Ohno (2002) formula but using PARAFAC components of heavy and light organic matter compounds from our samples instead of 2D windows. Finally, we evaluated TTi relevance as a transit time tracer by (i) performing a detailed analysis of its dynamic on a selected spring (Millet) and (ii) comparing its mean value over karst springs of the Fontaine de Vaucluse system.

2 Materials and methods

2.1 Study site

This study was carried out in the Vaucluse karst system (southeastern France) (Fig. 1). This hydrosystem, mainly composed of outcropping marine Cretaceous limestones, is unusual in terms of dimension and volume. Its main outlet, Fontaine de Vaucluse spring, has a mean flow rate of $23.3 \text{ m}^3 \text{ s}^{-1}$ (from January 1877 to June 2006; Cognard-Plancq et al., 2006), which is one of the highest in Europe. It is also characterized by a particularly thick unsaturated zone ($\sim 800 \text{ m}$). Monitoring of flows in its unsaturated zone at depths ranging from $\sim 30 \text{ m}$ to almost 500 m is made possible through the artificial galleries of the LSBB (<https://lsbb.cnrs.fr>, last access: 27 September 2022). Several outlets of less importance are also located on the recharge area of the Vaucluse karst system, the main ones being Millet, St Trinit, and Nesque springs (Table 1). The main karstification mechanism is epigenetic, but there is evidence of hypogenetic karstification at the southern edge of the Fontaine de Vaucluse system (Audra et al., 2011).

2.2 Sampling and fluorescence analysis methods

Bimonthly sampling of all flow points was performed during a 1-year monitoring period (June 2020 to October 2021). Measurements of major elements, TOC, and water stable isotopes were performed by UMR 1114 EMMAH with ion chromatography on the Dionex ICS-1100, Aurora 1030 TOC analyzer, and Picarro L2130-i, respectively. The excitation–emission matrix (EEM) and 2D spectra of organic matter fluorescence were analyzed at HydroSciences Montpellier using a spectrofluorometer (SHIMADZU RF-5301 PC; 150 W xenon lamp) (Serène et al., 2022). Wavelength windows for EEMs were $\lambda_{\text{ex}} = [220; 450] \text{ nm}$ and interval = 10 nm and $\lambda_{\text{em}} = [250; 550] \text{ nm}$ and interval = 1 nm . Wavelengths for the 2D spectrum were $\lambda_{\text{ex}} = 254 \text{ nm}$ and $\lambda_{\text{em}} = [220; 530] \text{ nm}$. The temperature was stabilized at 20°C in a bath with a thermostat. Slit widths of 15 nm were used for the monochromators with a fast default scan speed. The stability of the apparatus was checked based on the Raman peak on fresh MilliQ water excited at 348 nm .

Identification of natural organic matter components in our samples was performed by both manual and automatic procedures. Manual peak picking was performed on raw EEMs of over 10 % of representative samples of the dataset, leading to the identification of about 80 fluorophores corresponding to seven different components. EEMs were also treated thanks to R software and the staRdom package (Pucher et al., 2019). Each of the 289 EEMs was corrected with blank subtraction, Raman normalization (Lawaetz and Stedmon, 2009), and scattering removal (Lakowicz, 2006; Murphy et al., 2013). Removed scatter was interpolated with spline interpolation (Lee et al., 1997). PARAFAC modeling was then

performed to extract organic matter components thanks to the same software and package using non-negative constraints for all modes, following the method described by Andersen and Bro (2003).

2.3 Transit Time index (TTi) definition

Based on the fluorescence analysis of our samples, we propose the Transit Time index (TTi) which derives from the HIX definition of Ohno (2002) but differs by the analytic method of organic matter (2D vs 3D). TTi is thus the ratio of heavy organic matter (high-emission wavelengths, humic-like organic matter) to heavy and light organic matter (low-emission wavelengths, protein-like organic matter):

$$\text{TTi} = \frac{\text{humic-like}}{(\text{humic-like}) + (\text{protein-like})}, \quad (2)$$

where humic-like and protein-like parameters correspond to the sum of all compound weights of each type from the PARAFAC model. Unlike HIX, TTi considers the totality of fluorescent organic matter compounds in groundwater. TTi value close to 1 means that organic matter is composed of low digestible organic matter (humic-like), which indicates a relatively long transit time. On the other hand, TTi close to 0 means that organic matter is composed of highly digestible organic matter (protein-like), which indicates a very short transit time.

3 Results and discussion

3.1 Identification of organic matter compounds

3.1.1 2D spectra results

The emission wavelengths of windows used to compute HIX have been compared to 2D spectra of natural fluorescence of representative samples from our dataset (Fig. 2). As compared to the proposed windows, (i) the protein peak of the Millet spring sample only partially fits inside, and (ii) the 370 nm protein peak of the St Trinit spring sample is shifted towards longer wavelengths. In both cases, emission of fluorescence of protein organic matter components is not correctly considered by HIX calculation. Proposed fluorescence windows are thus not appropriate to characterize organic matter in groundwater. We hypothesize that this mismatch may be related to the fact that groundwater's organic matter is more digested than that of its own source, which is the soil.

3.1.2 PARAFAC model results

The resulting PARAFAC model managed with non-negative constraints contains four different components of organic matter. It was chosen for its explained variance of 0.9825 and its core consistency of 92.7 %, and it was checked thanks to

Table 1. Main characteristics of monitored flow points from Batiot (2002), Blondel (2008), Emblanch et al. (1998), Lastennet (1994), Ollivier (2019), and field observations. UZ is the unsaturated zone.

Spring	Catchment area	Karstification	UZ thickness	Lithology	Land use
Millet	~ 2.5 km ²	Complex karstification – anastomoses	Thick ~ 70 m	Cretaceous/Barremian limestones (marine)	Forest, lavender cultivation
St Trinit	~ 2 km ²	High degree, large karstic conduit	Thin ~ 10 to 20 m	Cretaceous/Aptian limestones (marine)	Anthropic activities, organic farming, town
La Nesque	~ 1 km ²	Low degree, conduits of centimetric scale at the outlet	Thin ~ 10 to 20 m	Marly limestones, Oligocene (lacustrine)	Lavender cultivation
Fontaine de Vaucluse	~ 1160 km ²	Variable but high on average	Very thick ~ 800 m	Cretaceous limestones (marine)	Cultivations, cities, forests
LSBB	≤ 1 km ²	Variable	35 à 518 m	Cretaceous limestones (marine)	Forest and cultivation

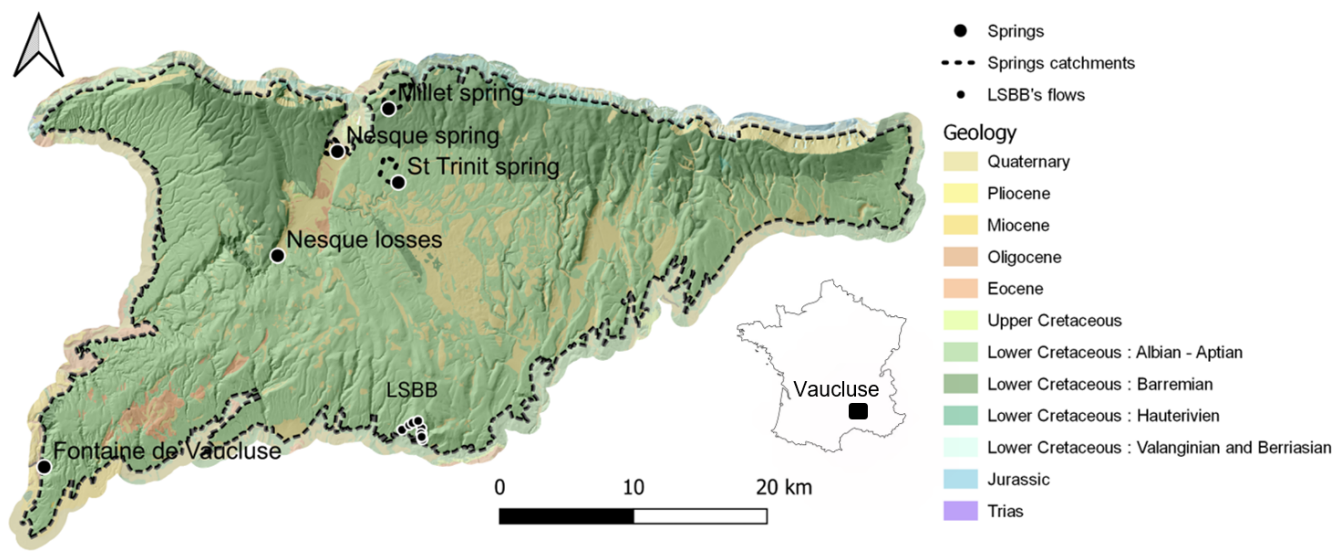


Figure 1. Location of monitored flow points on a 1 : 50 000 geological map (BD-CHARM) from BRGM and spring catchment delineation (based on geology and mass balance for Millet, St Trinit, and Nesque springs; from Ollivier (2019) for Fontaine de Vaucluse).

split-half analysis, Tucker’s congruency, plotting of components, and random initialization (Andersen and Bro, 2003). Three of the four identified components contain two close but distinguishable compounds (components 1, 2, and 4). PARAFAC components are in good agreement with manual peak picking performed on raw EEMs, compound 3 apart, which is affected by harmonics. Comparison with excitation–emission windows from the literature allows organic matter compounds represented by each component to be identified (Fig. 3).

Component 1 is typical of heavy compounds belonging to humic-like organic matter type (Blondel, 2008; Quiers et al., 2014). Component 2 is composed of two tryptophan-like compounds (Trp). Indeed, the compound with the longer excitation wavelength closely matches Trp 1 from Birdwell and Engel (2010), and the compound with the shorter excitation wavelength appears to be another declination of tryptophan-

like organic matter, different from Trp 2 from Birdwell and Engel (2010). Component 3 is consistent with P1 observation from Quiers et al. (2014). This compound lies close to Trp 2, but its emission wavelength is too high for it to belong to tryptophan-like organic matter. Quite surprisingly, it is far from P1 observation of Blondel (2008). We hypothesize that P1 was mistaken for tryptophan-like organic matter by Blondel (2008). Component 3 also lies far from the hand peak picking window of P1, probably because hand peak picking was performed on raw EEMs not yet corrected from harmonics. Component 4 contains one main compound which we assume to be tyrosine-like organic matter (Tyr) because it lies really close to the Tyr 1 observation of Mudarra et al. (2011). A second component with lower intensity may correspond to Tyr 2 of Mudarra et al. (2011).

The four components identified by PARAFAC modeling can thus be gathered into humic-like organic matter (compo-

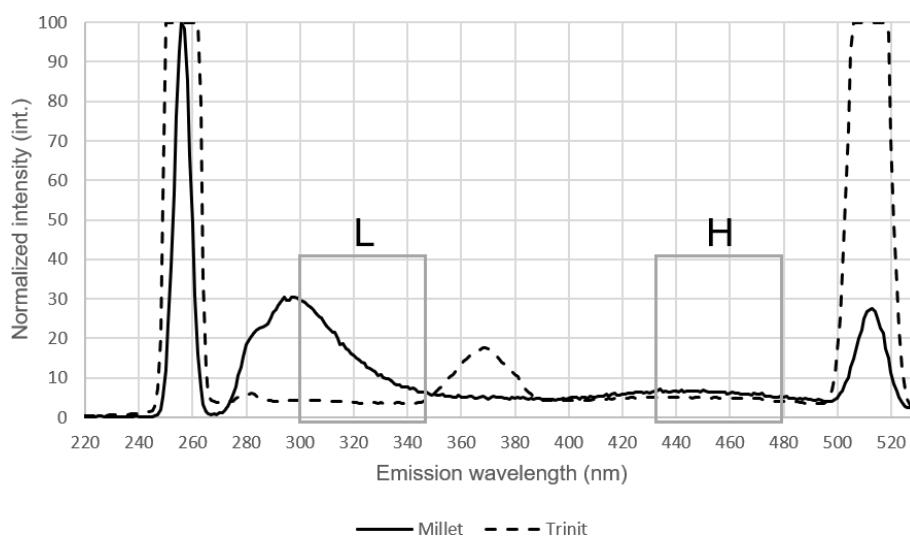


Figure 2. The 2D spectra at excitation wavelength 254 nm for two representative samples (Millet on 3 May 2021 and St Trinit on 1 February 2021). Comparison with Ohno (2002) H and L windows.

nent 1) and protein-like organic matter (components 2, 3, and 4). We also note that 2D spectra at 254 nm may accurately illustrate the maximum intensity of Trp2 and H2 but miss the maximum intensity of H1. Use of EEM instead of 2D spectra thus appears necessary to achieve the characterization of all the humic-like and protein-like compounds required for humification index calculation.

3.1.3 TTi application at Millet spring

3.1.4 Hydrodynamic and hydrochemical functioning of Millet spring

Descriptive statistics of major ions, TOC, electrical conductivity, humic-like and protein-like organic matter, TTi, standard deviation, and coefficient of variation are available in Table 2 and represented as time series in Fig. 4. These parameters were chosen for their ability to improve recharge and transit time knowledge on flows and springs of the Fontaine de Vaucluse system (Garry, 2007; Barbel-Périneau, 2013; Blondel, 2008). Silica and magnesium are two elements classically used as markers of the reserve and therefore are associated with a long transit time because of their slow solution kinetics (Lastennet and Mudry, 1997).

Discharge at Millet spring reacts sharply to rainfall events (Fig. 4) which indicates that the karst network is mature. Conversely, natural tracers such as $\delta^{18}\text{O}$ and major elements are not well correlated with discharge and have low-amplitude variations, highlighting the high mixing ability of the Millet system. It is particularly the case of $\delta^{18}\text{O}$, whose variations are close to detection limits. Such global hydrochemical stability suggests the presence of a storage zone in which the mixing of waters is particularly effective, which we relate to the structure of its karstification (anastomose).

Electrical conductivity correlates well with discharge, and the highest conductivities are reached during high discharge with a 2 to 4 d delay. This positive correlation between electrical conductivity and discharge is less usual, but it has also been observed in other karst springs of the Fontaine de Vaucluse system (Notre-Dame-des-Anges spring in Emblanch et al., 2006), other Mediterranean karst systems such as the Lez spring (Bicalho et al., 2012), or in Europe at Podstenjšek spring, Slovenia (Ravbar et al., 2011). This phenomenon may result from dilution of deep flows with recent water like in the Lez spring (Bicalho et al., 2012), a change in the catchment delineation that captures old water stored outside the usual catchment area (Ravbar et al., 2011), or a supply of water stored in the unsaturated zone (Emblanch et al., 2006).

At Millet spring, electrical conductivity is mainly carried by Ca^{2+} and HCO_3^- contents. Its increase at the beginning of flood events is caused by HCO_3^- increase, which indicates the arrival of water characterized by higher $p\text{CO}_2$ (see Fig. 4). $p\text{CO}_2$ has higher content in soil water because of biological respiration and organic matter decomposition. A $p\text{CO}_2$ increase in spring involves (i) a stronger influence of soil water which may be stored in the unsaturated zone or epikarst or (ii) a very fast infiltration supply. Case (i) is the most likely because case (ii) involves high organic matter content (TOC), while the increase of TOC corresponds to less than 0.6 mg L^{-1} .

Arrival of water associated with a short residence time is usually evidenced by TOC (Batiot et al., 2003). TOC is a natural tracer of fast infiltration, which decreases with increasing transit time. From a hydrodynamic point of view, Millet spring is a fast-reacting karstic system, and TOC is thus expected to increase sharply during flood events. Measured TOC does correlate with discharge, but it varies little and does not exceed 2 mg L^{-1} , showing evidence of a mix of dif-

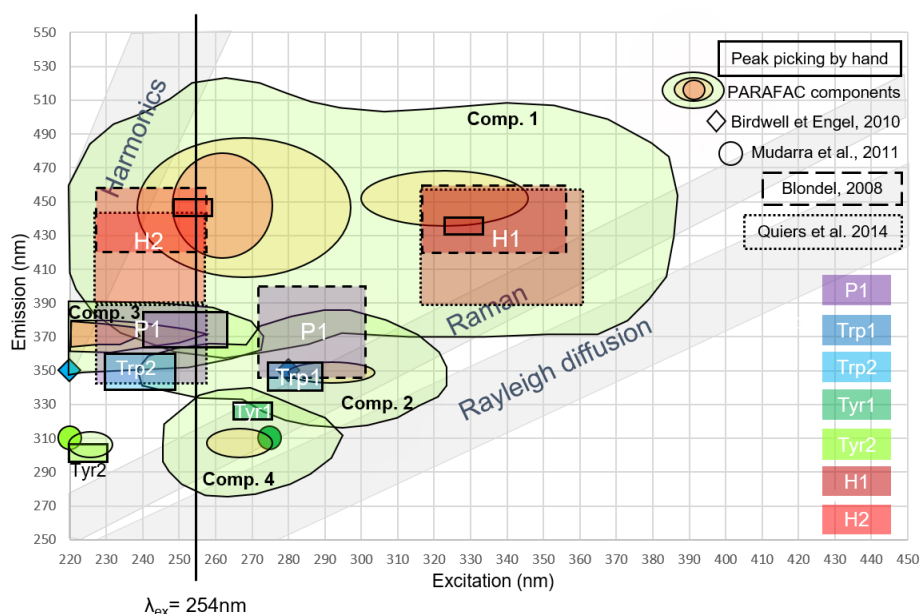


Figure 3. Comparison of organic matter component location in EEMs in literature and our study.

ferent water types. Stored water may have a lower TOC content in comparison with fresh water supply because of natural organic matter degradation. It thus appears that as TOC provides evidence of arrival of water with short transit times, its limits of sensitivity also seem to be reached.

3.1.5 Relation between TTi components and other variables

The correlation matrix presented in Fig. 5a shows a positive correlation between TTi and component 1 and anticorrelation with components 2, 3, and 4, which stems from the TTi formula. The anticorrelation is stronger with tyrosine due to its high digestibility, leading to a higher variability of its concentrations. Indeed, fluorescent organic matter digestibility decreases with increasing emission wavelength, and tyrosine has the lower one (Fig. 3). Components 2 and 3 are strongly correlated, caused by the similarity of their emission wavelength and thus of their degradation kinetics. The highest correlation of the first (humic-like) component is found with electrical conductivity and discharge. The humic-like component has the longest lifetime of all fluorescent organic matter because of its low digestibility, and it thus has the highest emission wavelength (Fig. 3). Humic-like organic matter is thus always present in the system as seen in Fig. 4 and thus may vary at the same low frequency as electrical conductivity and discharge, while protein-like organic matter, because of its short life duration, may vary at high frequency. TTi correlation with magnesium was expected because this tracer has increasing values with transit time like TTi. But TTi is surprisingly anticorrelated with SiO_2 . This anticorrelation is mainly supported by tyrosine variation. Usually,

rock dissolution is the main source of dissolved silica, inducing increasing contents with transit time. If so, SiO_2 would be correlated with TTi, magnesium, and electrical conductivity. At Millet, SiO_2 is anticorrelated with these elements and correlated with tyrosine, which has decreasing contents with increasing transit time, thus indicating similar SiO_2 and tyrosine kinetics, both coming from an organic source (soil). This hypothesis is validated by the high content of SiO_2 in Millet soil water (around 10 mg L^{-1} in November 2000; Batiot, 2002).

To characterize the source of the TTi signal, principal component analysis (PCA) was performed on 27 Millet spring samples with TTi, TTi components (Tyr, P1, H1, and H2), and other variables related to transit time (electrical conductivity, discharge, magnesium, and silica contents). Component 2 Trp was omitted because of its strong correlation with P1 (0.76, Fig. 5b) and its lower intensity, as seen in Fig. 3. The three principal axes of PCA explain about 73.2 % of the total variance. The first principal component (Dim. 1) represents 36.7 % of total variance, the second (Dim. 2) 25.2 %, and the third (Dim. 3) 11.3 %. They are carried by different variables as seen in Fig. 5b. PCA results are provided in Fig. 6.

The first dimension is negatively scored with tyrosine and SiO_2 and positively with Mg^{2+} and TTi. These variables have high-frequency variation in common. Indeed, tyrosine has the shorter lifetime duration of tested variables and is linked to silica. Its degradation kinetics is therefore very short, implying strong variations over time. TTi and magnesium are in the opposite direction. For TTi, it is because of its opposition to protein-like organic matter compounds, caused by its construction. For magnesium, this opposition is

Table 2. Descriptive statistics at Millet spring of major ions, TOC, electrical conductivity, humic-like and protein-like organic matter, and TTi. SD is standard deviation, and CoV is coefficient of variation, over the period June 2020 to October 2021 (29 samples).

Parameter	Unit	Min	Max	Mean value	SD	CoV (%)
TTi	–	0.11	0.93	0.41	0.19	46
Humic-like	intensity	0.05	3.97	1.17	0.09	8
Protein-like	intensity	0.44	0.75	0.61	0.84	138
CE	$\mu\text{S cm}^{-1}$	305.6	338.5	317.7	8.48	3
$\delta^{18}\text{O}$	‰	−8.96	−8.76	−8.89	0.05	−0.6
Mg^{2+}	mg L^{-1}	0.74	1.51	1.06	0.20	19
SiO_2	mg L^{-1}	5.45	7.62	7.00	0.53	8
TOC	mg L^{-1}	0.82	2.15	1.03	0.24	23
Cl^-	mg L^{-1}	1.38	2.38	1.86	0.28	15
NO_3^-	mg L^{-1}	0.39	2.5	1.11	0.45	40
SO_4^{2-}	mg L^{-1}	2.36	4.2	3.17	0.35	11

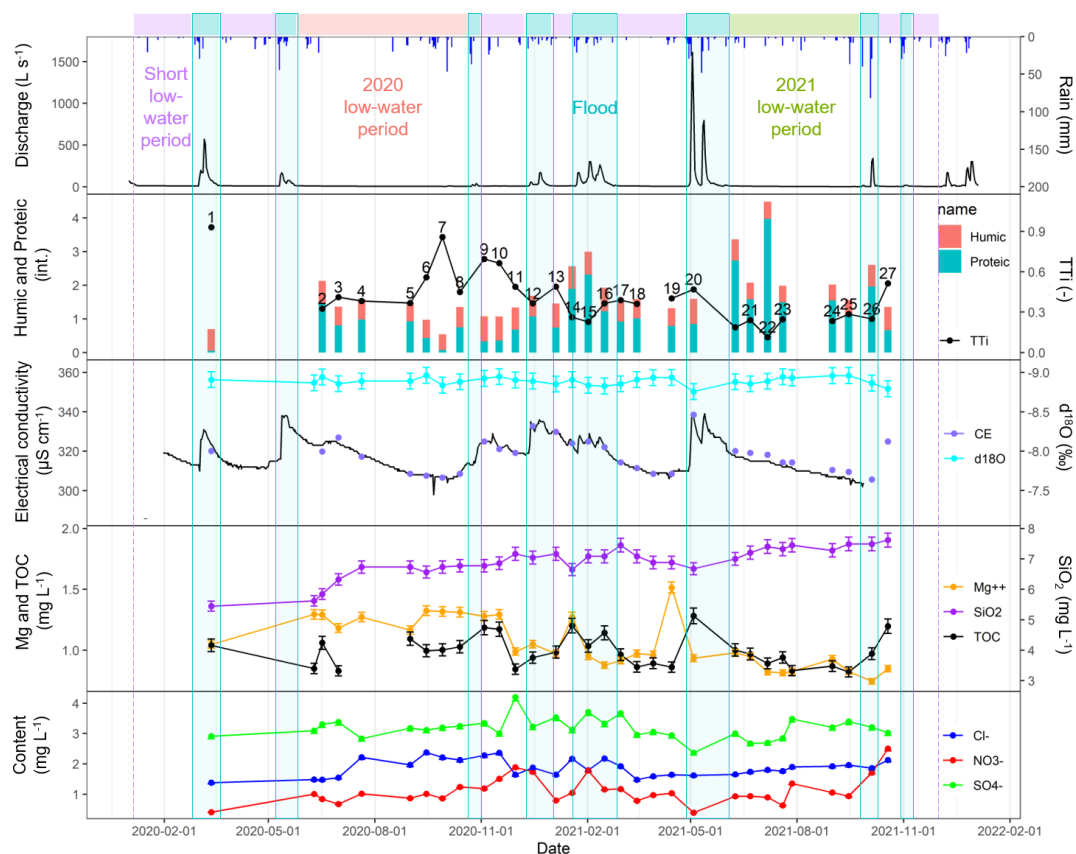


Figure 4. Millet spring time series of rain, discharge (Mazzilli et al., 2022), TTi, humic-like (component 1) and protein-like (sum of components 2, 3 and 4) fluorescent organic matter, continuous and punctual electrical conductivity, $\delta^{18}\text{O}$, $p\text{CO}_2$, and magnesium, silica, chloride, nitrate, and sulfate contents over the period from June 2020 to October 2021. Colors above the discharge plot and numbers on the TTi curve correspond to Fig. 6b.

caused by the dilution of stored water by freshwater supply. Dim. 1 thus corresponds to high-frequency variations led by rain events (daily scale) bringing fresh organic matter rich in tyrosine and SiO_2 and diluting stored water, implying magnesium decrease.

The second dimension is positively scored with electrical conductivity, discharge, and humic-like organic matter (component 1). These variables evolve at low frequency (monthly to seasonal scale), mainly due to the alternance of low- and high-flow periods. Positive correlation between humic-like

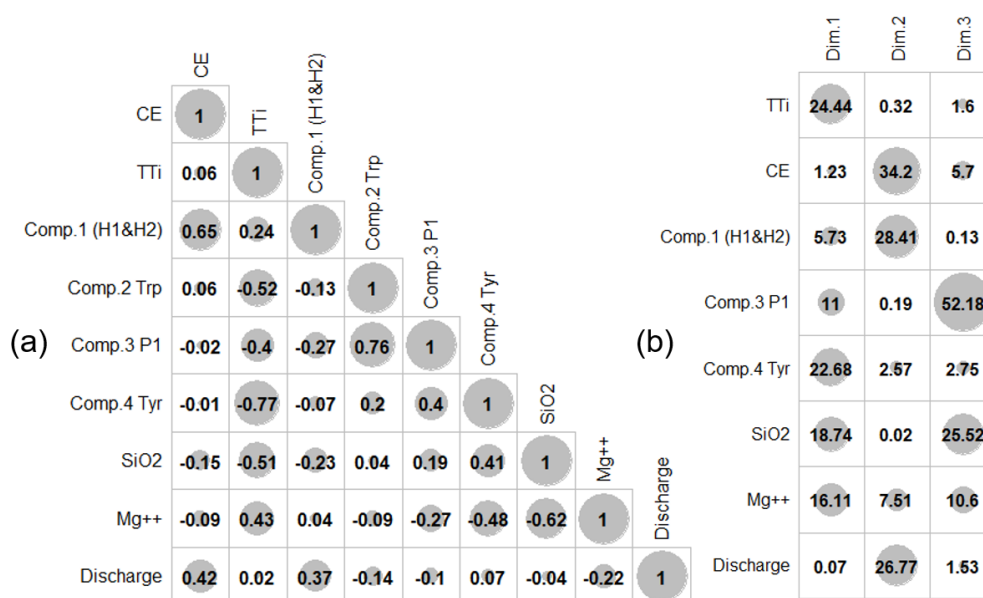


Figure 5. Correlation matrix of variables (a) and variable contributions to the three principal components of PCA (b).

organic matter, electrical conductivity, and discharge, while unexpected, may stem from the fact that as with TOC, humic-like organic matter results from a mix of stored and fresh water. Increase in humic-like organic matter can be caused by the arrival of (i) fresh water with high content of all types of organic matter and thus TOC content or of (ii) stored water with high relative humic-like organic matter content compared to the other organic compounds. Case (ii) seems the most likely because at Millet, the increase of humic-like is associated with a steady TOC content. This second dimension therefore seems to indicate a seasonal variation of humic-like organic matter content due to seasonal storage dynamics, which may induce a seasonal variation of TTI.

The third dimension is negatively scored with SiO₂ and positively with P1 and magnesium. In comparison with other variables, these two variables have intermediate-frequency variations. Indeed, P1 emission wavelength is between the emission wavelengths of humic-like organic matter and tyrosine (Fig. 3) and thus has an intermediate lifetime duration (from weeks to months). Magnesium is little explained by Dim. 3 (10.6 %), suggesting that a little part of magnesium has an organic source (soil). SiO₂ is in the opposite direction, which shows a part of its content coming from rock dissolution or mineralization.

Variation frequency can easily be linked with transit time because natural tracers of a precise range, must, by definition, vary in this range. Dim. 1 is thus susceptible to tracing a short transit time at daily scale, Dim. 2 a long transit time at monthly/seasonal scale, and Dim. 3 an intermediate transit time at weekly scale.

Projection of samples on the factor plane is consistent with the different ranges of transit time associated with PCA di-

mensions (Fig. 6b, d). Samples from the 2020 low-water period are mainly expressed by Dim. 2 and Dim. 3, corresponding to intermediate- to low-variation frequency. It is consistent because during low-flow periods, the expected transit time is long and may correspond to months. These samples are also, to a lesser extent, expressed by Dim. 1. For example, sample 5 has the lowest Dim. 1 score and corresponds to the reaction to a rain, whereas sample 7, which has the higher score, corresponds to a dry period during the low-flow period.

The 2021 low-water period has more frequent rainfall events. As compared to the 2020 low-water period, spread of samples from the 2021 low-water period is higher on factor planes 1 and 3. Samples from this period are mainly explained by Dim. 1 and 3, corresponding to intermediate and short transit time, in agreement with Millet's well karstified system inducing fast reactions. Flood event samples are expressed by Dim. 1 and Dim. 2 – high- and low-variation frequency. Samples close to Dim. 2 reflect the flushing out of stored water (piston effect – samples 12, 16, and 20); they correspond to the beginning of floods. Sample 1 is aligned with Dim. 1. It corresponds to freshwater arrival at the end of a flood, thus with short transit time (see time series in Fig. 4).

Short low-water period samples appear in no particular dimension because water age after a flood event may differ depending on intensity of previous floods and piston effect duration and also contain very recent water as seen in the case of the long-duration, 2021 rainy low water period.

Observation of sample projection on PCA results thus validates the accuracy of the identified dimensions and the viability of TTI components to illustrate different ranges of transit time at Millet karstic system. TTI is therefore able to

provide more information about the functioning of complex karstic systems, even in highly mixed systems like Millet.

3.1.6 Time variability of Transit Time index (TTi)

Lowest TTi values occur in low-flow periods: TTi is 0.3 on average during 2021 low-flow period and 0.5 on average during the 2020 low-flow period (Fig. 4). It is consistent with the relative transit times expected over these two periods based on magnesium contents (~ 1.3 in 2020 vs $\sim 0.8 \text{ mg L}^{-1}$ in 2021) and hydrometeorological conditions as rainfall is more uniformly distributed in time in the 2021 low-flow period than in the 2020 period.

TTi behavior during flood period is complex as it may correlate either (i) negatively (e.g., samples 12 and 15) or (ii) positively (e.g., samples 8–9 and 20) with discharge. Case (i) is expected when infiltrated fresh water, which is rich in organic matter (protein-like compounds), is dominant and thus yields a decrease in TTi. Case (ii) is unusual except at the early stage of high water when infiltrated water flushes out old water (piston effect). At later stages it may be related to the ratio of stored to fresh water being too high to induce a decrease in TTi, for example, in the case of short floods.

It thus appears that TTi is able to identify piston effects and also, as TOC, to identify a slight proportion of freshwater in a mix. However, TTi is more sensitive as seen by its punctual correlation with discharge (case (ii)) and its punctual uncorrelation with TOC as in samples 5 to 8 and 14 to 17 (Fig. 4).

Analysis of time variability of TTi at Millet spring thus (i) reinforces the consistency of TTi variations and (ii) indicates a better sensitivity of this marker than TOC to freshwater arrivals. Thanks to its higher sensitivity, TTi also allows for a better understanding of the Millet karstic system where other natural tracers fail.

3.2 Comparison of average TTi values of Vaucluse karst springs

Visual comparison of electrical conductivity, chloride, magnesium, nitrates, TOC, and TTi distributions from our dataset is provided in Fig. 7. TTi variability is higher than that of other elements at each monitored spring, which suggests that TTi is more sensitive. The TTi median value increases from St Trinit to Nesque springs via Millet spring.

The spring with the lowest TTi values (St Trinit) has the highest karstification level, thinnest unsaturated zone, and highest nitrate and chloride contents, which are compatible with shorter median transit times. As compared to St Trinit, Millet has lower and less variable chloride and nitrate contents and less variable TOC. The anastomose karst network is assumed to provide a mixing effect of infiltrated water. We thus suppose that this system is less affected by fast infiltration than St Trinit. The highest TTi values are found at the Nesque spring, which is the less karstified system. The

relative distribution of TTi values at St Trinit, Millet, and Nesque springs is therefore consistent with the expected behavior of a transit time indicator, depending on their karstification type and thus on their hydrodynamical and hydrochemical responses. The median value of TTi at Fontaine de Vaucluse spring is similar to that of Nesque spring. However, the mean water transit time at Fontaine de Vaucluse spring is expected to be significantly higher than that of Nesque spring because it is the outlet of a wider system with thicker saturated and unsaturated zones. This inconsistency is related to the relatively short timescale of transit times covered by TTi. Maturation of organic matter components constituting TTi is almost complete after 6 months (TOC degradation; Batiot, 2002), while the water flowing from the Fontaine de Vaucluse spring is a mixture of water with a long residence time (several years) and freshwater coming from rapid infiltrations through the shortcuts existing in the underground infiltration network (Margrta et al., 1970). Transit times of most Fontaine de Vaucluse samples are thus probably out of the range of relevance of TTi to quantitatively identify transit time values. However, TTi as it is more sensitive may identify freshwater arrivals in the mix of waters flowing at the Fontaine de Vaucluse spring during flood events.

3.3 Way forward towards a transferable qualitative tracer and a quantitative approach

As demonstrated in Sect. 3.2 and 3.3, TTi is a new tool which seems to have a real potential to be a qualitative natural tracer of transit time. To make TTi a quantitative natural tracer of transit time, several avenues have to be explored, such as an artificial tracer test, the use of radiogenic isotopes, or the study of organic matter degradation kinetics.

The artificial tracer test consists in injecting a tracer in a place known for its strong and rapid connectivity with the hydrosystem and in monitoring its restitution at a presumed outlet. It thus informs about the existence of a path between the injection point and the outlet and provides an estimate of the transit time between the two. A set of several artificial tracer tests may provide enough transit time values to quantitatively connect TTi with transit time. However, to compare TTi with artificial tracer tests, it is necessary to check that they provide the same information. An artificial tracer test with uranine, tryptophan, and humic-like organic matter performed by Frank et al. (2020) in a karst system shows that uranine has the same transport properties as tryptophan but not as humic-like organic matter. It therefore seems that artificial tracer tests may not correctly illustrate the behavior of all the organic matter compounds involved in TTi. Moreover, not all artificial tracers may be compatible with simultaneous analysis of natural fluorescence of organic matter. For example, widely used uranine may overlay the natural fluorescence of protein-like compounds (P1, tyrosine-like). Indeed, the quantification of artificial tracers in a sample is performed by spectrofluorescence, exactly like the quantifi-

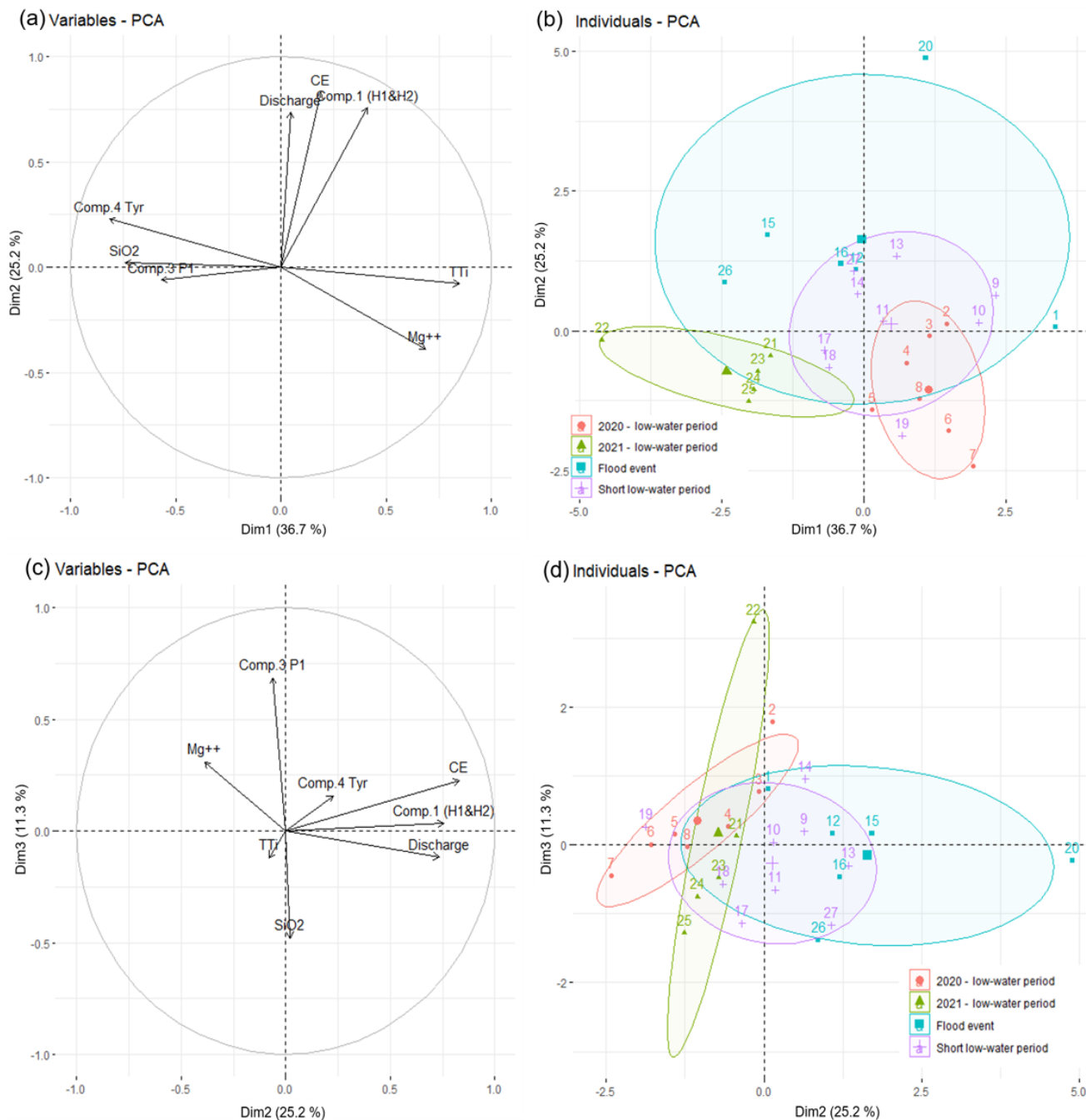


Figure 6. PCA performed with Millet spring samples thanks to the following variables: TTI components, TTI, SiO_2 , Mg^{2+} , electrical conductivity, and discharge. Dimensions 1 and 2 are presented in (a) and (b) and dimensions 2 and 3 in (c) and (d). Panels (a) and (c) show variables. Panels (b) and (d) show individuals, where point color corresponds to hydrodynamic periods (see Fig. 4) and point label to sample number (see Fig. 4), and the confidence ellipse is 70 %.

cation of fluorescent organic matter compounds needed to calculate TTI. Some artificial tracers have emission and excitation wavelengths in the same area of the EEM of some organic compounds and may thus hide the natural signal of organic matter. Use of such tracers would not be compatible with quantification of TTI. Furthermore, some organic matter

compounds have the ability to adsorb themselves to artificial tracers molecules, which would interfere with the TTI signal. Selection of an artificial tracer in such an experiment will therefore have to be taken with caution. A more fundamental remark is that TTI is related to residence time of a mix of water originating from different paths within the aquifer,

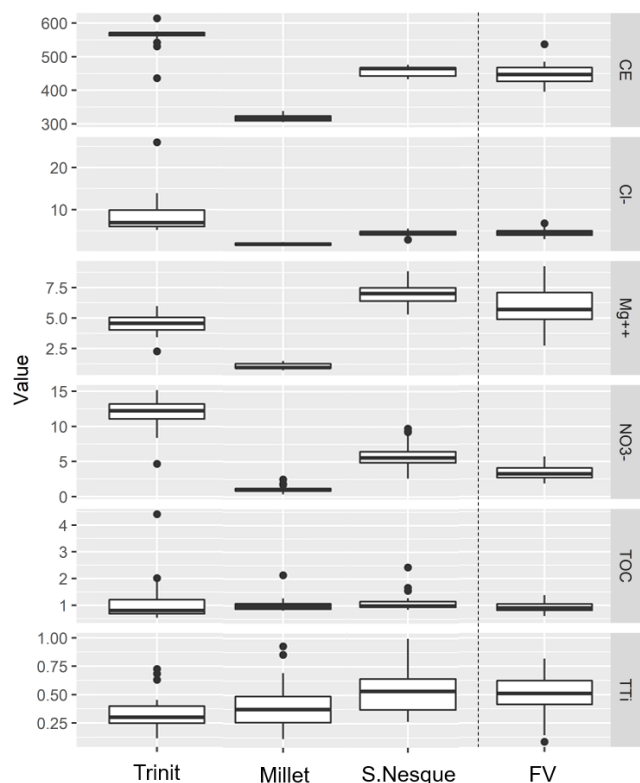


Figure 7. Box plots of electrical conductivity, chlorides, magnesium, nitrates, TOC, and TTI of Fontaine de Vaucluse (FV, 25 samples), Millet (27 samples), Nesque (S. Nesque, 29 samples), and St Trinit (Trinit, 29 samples) springs.

while artificial tracers only trace the fastest circulations due to injection through well-connected conduits. This observation raises the question of the comparability of transit time evidenced by both methods. In addition, the presence of possible injection points is not guaranteed for all hydrosystems. For example, no possible injection point could be identified at Millet spring for now. As a conclusion, artificial tracing may be a good candidate to identify fast infiltration, as long as no interference is possible (fluorescein usage), and the transit time obtained is not mistaken for residence time.

A second approach to establish a quantitative link between TTI and residence time is the use of radiogenic isotopes like beryllium-7, radium, or radon-222. Price apart, the use of radiogenic isotopes may be problematic because of the volume of water needed for analysis which reaches several hundred of liters (e.g. 500 L for beryllium-7; Frey et al., 2011), which reserves its use for water flow points with sufficient discharge for sampling to be performed within a sensible timescale. The sampling time for radiogenic isotopes from some flow points in our study can be several days. Even quite important springs may reach low discharges that prevent such analysis during low flows. Nevertheless, radiogenic isotopes can be relevant for linking TTI to transit time values for samples from springs and flows with a sufficient discharge.

The study of the degradation rate of organic matter is also necessary to transform TTI as a quantitative natural tracer because it may help to estimate the duration life of each kind of organic matter in the natural environment and therefore inform on transit time. In soil, the biodegradation of labile organic matter was estimated from 2 to 5 d, while the stable organic matter ranges from 0.2 to 8.6 years (half-life from Kalbitz et al., 2003). But the biological activity is more important in soil than in groundwater. Therefore, these lifetimes obtained in soil are probably shorter than those in groundwater. A recent paper based on the improvement of the understanding of dissolved organic matter degradation in groundwater pointed out the lack of knowledge on this subject (McDonough et al., 2022). As little is known about the behavior of DOM in natural waters, even less is known about fluorescent organic matter, which is a small part of the DOM. The paper cited previously therefore discusses a very long transit time (several years), while we are considering a very short one (weeks to months). Nevertheless, interesting studies were performed about fluorescent organic matter degradation kinetics in soils, or in wastewater, testing different water treatment (De Willigen et al., 2008; Conant et al., 2011; Baldock et al., 2021; Choi et al., 2017; Guo et al., 2020). These studies are difficult to perform, but they could be adapted to natural water in order to improve fluorescent organic matter natural degradation and therefore help in the development of TTI.

The transferability of TTI in different pedoclimatic and anthropogenic contexts may also be questioned. Indeed, anthropic activities and seasonality may affect TTI through organic matter production and degradation:

- Fluorescent organic matter mainly comes from vegetation related to the plant cycle. As the vegetation changes with the seasons, the organic matter supply changes as well, at least in terms of quantity. Seasonality does not significantly affect organic matter composition, as demonstrated in Musadji et al. (2019). Anthropic activities such as land use or wastewater infiltration within the hydrosystem can affect both quantity and types of organic matter compounds because they involve input of external organic matter to the system. The influence of anthropic activity on the type of organic matter compounds may be significant and may vary over time. Moreover, the anthropic activities and the vegetation may vary from one site to another due to different pedoclimatic conditions and complicate the transposition of a quantitative TTI.

As TTI is a ratio of different organic matter compounds, it is calculated independent of the absolute amount of organic matter. Possible bias may appear when very low input of a specific type of organic matter results in DOM content below the detection limits. In this case, degradation is overestimated, which may impact the quantitative relation between TTI and transit time. Overall, we

expect T*Ti* to be little affected by seasonal variations of productivity, even if it is quantitatively linked to residence times. As T*Ti* is a ratio, a regular and constant supply of anthropic organic matter may not impact its variation. But in contrast, a punctual supply of humic or protein-like organic matter may result in an over- or underestimation of T*Ti*.

- The degradation of organic matter involves interactions with biocenose. Degradation occurs at different rates depending on the type of organic matter compounds and on the biodiversity and microbial activity of the soil. The latter may vary throughout seasons and with anthropic activities because of varying factors such as sunlight duration, moisture rate, temperature, climate, or pesticide use.

Variation in space and time in organic matter composition and degradation rate may thus stem from either anthropic or natural factors. Influence of anthropic compounds can be circumvented by careful identification and separation of PARAFAC components. Variation in organic matter composition and degradation kinetics in different pedoclimatic contexts is not an obstacle to the qualitative use of T*Ti* but may be a serious limitation to the transferability of a quantitative link between T*Ti* and residence time. Variation in organic matter degradation kinetics with time on the same hydrosystem throughout the year is questionable, but it is beginning to be studied, as shown by McDonough et al. (2022). A detailed study of the composition of organic matter source in soil and of its future in groundwater through lab tests may provide valuable elements to estimate the lifetime of fluorescent compounds in hydrosystems and thus to quantitatively link T*Ti* with transit time.

4 Conclusions

Groundwater from karst aquifers is an important resource for drinking water supply in the world (Stevanović, 2019). Soils from carbonate aquifers are generally poorly developed, which, combined with the rapidity of groundwater fluxes within karst conduits, explains the vulnerability of these aquifers to contamination. To face the challenge of the protection of karst water resources, several specific hydro-geochemical tracers have been developed by the community to characterize the different types of fluxes and recharge. One of the main current challenges is to develop natural tracers able to estimate water transit times for short time ranges of the order of 0 to 6 months. The main purpose of this work was to study the potential of the ratio of heavy- to light-weight organic compounds (HIX) as a natural tracer of short transit time in karst systems with a strong fast infiltration component in order to characterize the vulnerability of the aquifer.

Critical analysis of former studies showed that although the link between HIX and transit time seems consistent, the whole methodological approach needed to be consolidated. Natural fluorescence from 289 groundwater samples from four springs and 10 flow points located in the unsaturated zone of the Vaucluse karst system was characterized by parallel factor analysis (PARAFAC) of the EEM, thus (i) allowing for the identification of main fluorescent compounds of sampled groundwater and (ii) evidencing the inadequacy of HIX emission windows to characterize groundwater organic matter. We then proposed a new humification index called the Transit Time index (T*Ti*) based on the Ohno (2002) formula but using 3D PARAFAC components of heavy and light organic matter instead of 2D windows.

Finally, we evaluated T*Ti* relevance as a potential transit time tracer by (i) performing a detailed analysis of its dynamics on a selected spring (Millet spring) and (ii) comparing its mean value over karst springs of the Fontaine de Vaucluse system. Principal component analysis (PCA) of T*Ti*, T*Ti* components, and other hydrochemical parameters monitored at Millet spring put in relief the timescales of variability associated with the different organic matter compounds, which we relate to their digestibility. PCA results also provided evidence that T*Ti* can detect a small proportion of fast infiltration water within a mix, while other natural tracers of transit time provide no or less sensitive information. Relative distribution of T*Ti* at monitored karst springs is also consistent with relative transit times expected for small-scale, short average transit time systems. T*Ti* is therefore consistent with other natural tracers of transit time and provides qualitative complementary results. This qualitative approach of transit time based on T*Ti* is transferable to other karst sites, even in the case of anthropic contamination, thanks to PARAFAC modeling.

To be a quantitative tracer of water transit time, T*Ti* needs to be linked with other tools providing quantitative approaches such as radiogenic isotopes, artificial tracer tests, or experimental studies of the degradation kinetics of organic matter. Transferability of the quantitative relation between T*Ti* and transit time from one karst system to another may however be challenging because of organic matter supply variability, which depends on the hydro-pedoclimatic context and anthropic activities.

Code availability. The code is not publicly accessible as it was built following the steps of the package developer available here: https://cran.r-project.org/web/packages/staRdom/vignettes/PARAFAC_analysis_of_EEM.html (last access: 27 October 2021).

Data availability. Discharge time series of Millet spring used in this study are available at <https://doi.org/10.15148/bbae7eab-8abd-40d9-834e-9a0683e59da5> (Mazzilli et al., 2022).

For all the springs, chemical parameters are available at <https://doi.org/10.15148/7b94438a-7bb2-4382-bb25-a4a0c3fdc5d7> (SNO KARST, 2021), and the raw excitation–emission matrix of organic matter fluorescence is available at <https://doi.org/10.15148/8d6104e1-ae78-4b4e-8e50-198ccc5b19c9> (Serène et al., 2022).

Author contributions. MB and the SMBS (<https://www.lasorgue.fr/>, last access: 27 September 2022) took water samples that were analyzed for major elements, TOC, and water stable isotopes by MB, JD, and RS and for fluorescence of organic matter by LS. Formal data analysis was performed by LS and NM. CBG, CE, NM, and LS provided critical feedback and helped to shape the research and the analysis. GM acquired funding. LS prepared the manuscript with contributions from all co-authors.

Competing interests. The contact author has declared that none of the authors has any competing interests.

Disclaimer. Publisher's note: Copernicus Publications remains neutral with regard to jurisdictional claims in published maps and institutional affiliations.

Acknowledgements. This work was performed within the framework of the FDV/LSBB observation site, which is part of OZ-CAR (French network of Critical Zone observatories), SNO KARST (French observatory network, <https://sokarst.org/>, last access: 27 September 2022) initiative of INSU/CNRS, which seeks to support knowledge sharing and promote cross-disciplinary research on karst systems, and of the H+ observatory network. The authors would like to express their gratitude to the LSBB team for their technical and logistic help. A special acknowledgement is given to SIAEPA from the Sault region and Veolia for giving us access to Nesque spring.

Financial support. This research has been supported by Total (grant no. 187737) and the Montpellier Université d'Excellence (GAIA competition 2019).

Review statement. This paper was edited by Zhongbo Yu and reviewed by Weiquan Dong and one anonymous referee.

References

- Andersen, C. M. and Bro, R.: Practical aspects of PARAFAC modelling of fluorescence excitation–emission data, *J. Chemom.*, 17, 200–215, <https://doi.org/10.1002/cem.790>, 2003.
- Audra, P., Bigot, J. Y., Camus, H., Gauchon, C., and Wienin, M.: La grotte-mine du Piei (Lagnes, Vaucluse), paléokarst hypogène à remplissage de minerai de fer oxydé, *Karstologia*, 58, 1–14, 2011.
- Baker, A. and Lamont-Black, J.: Fluorescence of dissolved organic matter as a natural tracer of ground water, *Ground Water*, 39, 745, <https://doi-org.ezpum.scdi-montpellier.fr/10.1111/j.1745-6584.2001.tb02365.x>, 2001.
- Barbel-Périneau, A.: Caractérisation du fonctionnement de la zone non saturée des aquifères karstiques: Approche directe par études hydrodynamiques et hydrochimiques sur le Bassin de Recherche, d'Expérimentation et d'Observation de Fontaine de Vaucluse – Laboratoire Souterrain à Bas Bruit de Rustrel – Pays d'Apt, PhD thesis, Université d'Avignon et des Pays de Vaucluse, 30, 22, 2179, <https://tel.archives-ouvertes.fr/tel-00990290> (last access: 10 May 2022), 2013.
- Batiot, C.: Etude expérimentale du cycle du carbone en régions karstiques: apport du carbone organique et du carbone minéral à la connaissance hydrogéologique des systèmes, PhD thesis, Université d'Avignon et des Pays de Vaucluse, France, <https://www.theses.fr/2002AVIG0029> (last access: 10 May 2022), 2002.
- Batiot, C., Liñán, C., Andreo, B., Emblanch, C., Carrasco, F., and Blavoux, B.: Use of Total Organic Carbon (TOC) as tracer of diffuse infiltration in a dolomitic karstic system: The Nerja Cave (Andalusia, southern Spain), *Geophys. Res. Lett.* 30, 2179, <https://doi.org/10.1029/2003GL018546>, 2003.
- Bicalho, C. C., Batiot-Guilhe, C., Seidel, J. L., Van Exter, S., and Jourde, H.: Geochemical evidence of water source characterization and hydrodynamic responses in a karst aquifer, *J. Hydrol.*, 450, 206–218, 2012.
- Birdwell, J. E. and Engel, A. S.: Characterization of dissolved organic matter in cave and spring waters using UV–Vis absorbance and fluorescence spectroscopy, *Org. Geochem.* 41, 270–280, <https://doi.org/10.1016/j.orggeochem.2009.11.002>, 2010.
- Blondel, T.: Expérimentation et application sur les sites du Laboratoire Souterrain à Bas Bruit (LSBB) de Rustrel – Pays d'Apt et de Fontaine de Vaucluse, PhD thesis, Université d'Avignon et des Pays de Vaucluse, <https://www.theses.fr/2008AVIG0044> (last access: 10 May 2022), 2008.
- Blondel, T., Emblanch, C., Batiot-Guilhe, C., Dudal, Y., and Boyer, D.: Punctual and continuous estimation of transit time from dissolved organic matter fluorescence properties in karst aquifers, application to groundwaters of “Fontaine de Vaucluse” experimental basin (SE France), *Environ. Earth Sci.* 65, 2299–2309, <https://doi.org/10.1007/s12665-012-1562-x>, 2012.
- Choi, Y. Y., Baek, S. R., Kim, J. I., Choi, J. W., Hur, J., Lee, T. U., Park, C. J., and Lee, B. J.: Characteristics and biodegradability of wastewater organic matter in municipal wastewater treatment plants collecting domestic wastewater and industrial discharge, *Water*, 9, 409, <https://doi.org/10.3390/w9060409>, 2017.
- Cognard-Plancq, A.-L., Gevaudan, C., and Emblanch, C.: Historical monthly rainfall–runoff database on Fontaine de Vaucluse karst system: a review and lessons, *IIIe Symposium International Sur le Karst “Groundwater in the Mediterranean Countries”*, 465–475, 2006.

- Conant, R. T., Ryan, M. G., Ågren, G. I., Birge, H. E., Davidson, E. A., Eliasson, P. E., Evans, S. E., Frey, S. D., Giardina, C. P., Hopkins, F. M., Hyvönon, R., Kirschbaum, M. U. F., Lavallee, J. M., Leifeld, J., Parton, W. J., Steinweg, J. M., Wallenstein, M. D., Wetterstedt, A. M., and Bradford, M. A.: Temperature and soil organic matter decomposition rates—synthesis of current knowledge and a way forward, *Glob. Change Biol.*, 17, 3392–3404, <https://doi.org/10.1111/j.1365-2486.2011.02496.x>, 2011.
- De Willigen, P., Janssen, B. H., Heesmans, H. I. M., Conijn, J. G., Velthof, G. L., and Chardon, W. J.: Decomposition and accumulation of organic matter in soil; comparison of some models (No. 1726), *Alterra*, ISSN 1566-7197, 2008.
- Emblanch, C., Blavoux, B., Puig, J. M., and Couren, M.: Le marquage de la zone non saturée du karst à l'aide du Carbone 13: The use of carbon 13 as a tracer of the karst unsaturated zone, *Comptes-Rendus Séances Académie Sci. Séries IIA-Earth and Planetary Science*, 327–332, 1998.
- Emblanch, C., Charmoille, A., Jimenez, P., Andreo, B., Mudry, J., Bertrand, C., Batiot-Guilhe, C., and Lastennet, R.: Variabilité du type et de la qualité de l'information issue du traçage naturel en fonction des caractéristiques des systèmes étudiés, Quelques exemples français et espagnols, in: *Proceedings of the 8th Conference on Limestone Hydrogeology*, Neuchâtel, 101–104, 2006.
- Ewald, M., Berger, P., and Visser, S. A.: UV-visible absorption and fluorescence properties of fulvic acids of microbial origin as functions of their molecular weights, *Geoderma*, 43, 11–20, [https://doi.org/10.1016/0016-7061\(88\)90051-1](https://doi.org/10.1016/0016-7061(88)90051-1), 1988.
- Frank, S., Goepfert, N., and Goldscheider, N.: Field tracer tests to evaluate transport properties of tryptophan and humic acid in karst, *Groundwater*, 59, 59–70, <https://doi.org/10.1111/gwat.13015>, 2021.
- Frey, S., Kuells, C., and Schlosser, C.: New Hydrological Age-Dating techniques using cosmogenic radionuclides Beryllium-7 and Sodium-22, *IAEA-CN-186*, 2011.
- Garry, B.: Etude des processus d'écoulements de la zone non saturée pour la modélisation des aquifères karstiques – Expérimentation hydrodynamique et hydrochimique sur les sites du Laboratoire Souterrain à Bas Bruit (LSBB) de Rustrel et de Fontaine de Vaucluse, PhD thesis, Université d'Avignon et des Pays de Vaucluse, <https://www.theses.fr/2007AVIG0038> (last access: 10 May 2022), 2007.
- Guo, Y., Niu, Q., Sugano, T., and Li, Y. Y.: Biodegradable organic matter-containing ammonium wastewater treatment through simultaneous partial nitrification, anammox, denitrification and COD oxidization process, *Sci. Total Environ.*, 714, 136740, <https://doi.org/10.1016/j.scitotenv.2020.136740>, 2020.
- Kalbitz, K., Schmerwitz, J., Schwesig, D., and Matzner, E.: Biodegradation of soil-derived dissolved organic matter as related to its properties, *Geoderma*, 113, 273–291, [https://doi.org/10.1016/S0016-7061\(02\)00365-8](https://doi.org/10.1016/S0016-7061(02)00365-8), 2003.
- Lakowicz, J. R.: Principles of fluorescence spectroscopy, 3 Edn. Springer, New York, ISBN: 978-0-387-31278-1, 2006.
- Lapworth, D. J., Goody, D. C., Butcher, A. S., and Morris, B. L.: Tracing groundwater flow and sources of organic carbon in sandstone aquifers using fluorescence properties of dissolved organic matter (DOM), *Appl. Geochem.*, 23, 3384–3390, <https://doi.org/10.1016/j.apgeochem.2008.07.011>, 2008.
- Lastennet, R.: Rôle de la zone non saturée dans le fonctionnement des aquifères karstiques: approche par l'étude physico-chimique et isotopique du signal d'entrée et des exutoires du massif du Ventoux (Vaucluse), PhD thesis, Université d'Avignon et des Pays du Vaucluse, Avignon, France, <https://www.theses.fr/1994AVIG0018> (last access: 10 May 2022), 1994.
- Lastennet, R. and Mudry, J.: Role of karstification and rainfall in the behavior of a heterogeneous karst system, *Environ. Geol.*, 32, 114–123, 1997.
- Lawaetz, A. J. and Stedmon, C. A.: Fluorescence Intensity Calibration Using the Raman Scatter Peak of Water, *Appl. Spectrosc.*, 63, 936–940, <https://doi.org/10.1366/000370209788964548>, 2009.
- Lee, S., Wolberg, G., and Shin, S. Y.: Scattered data interpolation with multilevel B-splines, *IEEE T. Vis. Comput. Graph.*, 3, 228–244, <https://doi.org/10.1109/2945.620490>, 1997.
- Malik, P., Švasta, J., Michalko, J., and Gregor, M.: Indicative mean transit time estimation from $\delta^{18}\text{O}$ values as groundwater vulnerability indicator in karst-fissure aquifers, *Environ. Earth Sci.*, 75, 988, <https://doi.org/10.1007/s12665-016-5791-2>, 2016.
- Margrita, R., Evin, J., Flandrin, J., and Paloc, H.: Contribution des mesures isotopiques à l'étude de la Fontaine de Vaucluse, *AIEA (Vienna) SM*, 129, 333–348, 1970.
- Mazzilli, N., Cinkus, G., Masseron, L., and Emblanch, C.: Discharge time series for Millet spring (fontaine de Vaucluse karst system), *OSU OREME*, [data set], <https://doi.org/10.15148/bbae7eab-8abd-40d9-834e-9a0683e59da5>, 2022.
- McDonough, L. K., Andersen, M. S., Behnke, M. I., Rutledge, H., Oudone, P., Meredith, K., O'Carroll, D. M., Santos, I. R., Marjo, C. E., Spencer, R. G. M., McKenna, A. M., and Baker, A.: A new conceptual framework for the transformation of groundwater dissolved organic matter, *Nat. Commun.*, 13, 2153, <https://doi.org/10.1038/s41467-022-29711-9>, 2022.
- Mobed, J. J., Hemmingsen, S. L., Autry, J. L., and McGown, L. B.: Fluorescence Characterization of IHSS Humic Substances: Total Luminescence Spectra with Absorbance Correction, *Environ. Sci. Technol.*, 30, 3061–3065, <https://doi.org/10.1021/es960132l>, 1996.
- Mudarra, M., Andreo, B., and Baker, A.: Characterisation of dissolved organic matter in karst spring waters using intrinsic fluorescence: Relationship with infiltration processes, *Sci. Total Environ.*, 409, 3448–3462, <https://doi.org/10.1016/j.scitotenv.2011.05.026>, 2011.
- Murphy, K. R., Stedmon, C. A., Graeber, D., and Bro, R.: Fluorescence spectroscopy and multi-way techniques, *PARAFAC*, *Anal. Methods*, 5, 6557, <https://doi.org/10.1039/c3ay41160e>, 2013.
- Musadji, N. Y., Lemée, L., Caner, L., Porel, G., Poinot, P., and Geffroy-Rodier, C.: Spectral characteristics of soil dissolved organic matter: Long-term effects of exogenous organic matter on soil organic matter and spatial-temporal changes, *Chemosphere*, 27, 104665, <https://doi.org/10.1016/j.chemosphere.2019.124808>, 2019.
- Musgrove, M., Solder, J. E., Opsahl, S. P., and Wilson, J. T.: Timescales of water-quality change in a karst aquifer, south-central Texas, *J. Hydrol. X*, 4, 100041, <https://doi.org/10.1016/j.hydroa.2019.100041>, 2019.
- Ohno, T.: Fluorescence Inner-Filtering Correction for Determining the Humification Index of Dissolved Organic Matter, *Environ. Sci. Technol.*, 36, 742–746, <https://doi.org/10.1021/es0155276>, 2002.

- Ollivier, C.: Caractérisation et spatialisation de la recharge des hydrosystèmes karstiques: Application à l'aquifère de Fontaine de Vaucluse, France, PhD thesis, Université d'Avignon, <https://www.theses.fr/2019AVIG0056> (last access: 10 May 2022), 2020.
- Pérotin, L., de Montety, V., Ladouche, B., Bailly-Comte, V., Labasque, T., Vergnaud, V., Muller, R., Champollion, C., Tweed, S., and Seidel, J.-L.: Transfer of dissolved gases through a thick karstic vadose zone – Implications for recharge characterisation and groundwater age dating in karstic aquifers, *J. Hydrol.*, 601, 126576, <https://doi.org/10.1016/j.jhydrol.2021.126576>, 2021.
- Pronk, M., Goldscheider, N., and Zopfi, J.: Microbial communities in karst groundwater and their potential use for biomonitoring, *Hydrogeol. J.*, 17, 37–48, <https://doi.org/10.1007/s10040-008-0350-x>, 2009.
- Pucher, M., Wünsch, U., Weigelhofer, G., Murphy, K., Hein, T., and Graeber, D.: staRdom: Versatile Software for Analyzing Spectroscopic Data of Dissolved Organic Matter in R, *Water*, 11, 2366, <https://doi.org/10.3390/w11112366>, 2019.
- Quiers, M., Batiot-Guilhe, C., Bicalho, C. C., Perrette, Y., Seidel, J.-L., and Van Exter, S.: Characterisation of rapid infiltration flows and vulnerability in a karst aquifer using a decomposed fluorescence signal of dissolved organic matter, *Environ. Earth Sci.*, 71, 553–561, <https://doi.org/10.1007/s12665-013-2731-2>, 2014.
- Ravbar, N., Engelhardt, I., and Goldscheider, N.: Anomalous behaviour of specific electrical conductivity at a karst spring induced by variable catchment boundaries: the case of the Podstenjšek spring, Slovenia, *Hydrol. Proc.*, 25, 2130–2140, 2011.
- Serene, L., Batiot-Guilhe, C., Emblanch, C., Mazzilli, N., and Massonat, G.: Natural fluorescence of organic matter excitation-emission matrix (EEM) of underground water from Fontaine de Vaucluse system (2020 to 2021), OSU OREME, [data set], <https://doi.org/10.15148/8d6104e1-ae78-4b4e-8e50-198ccc5b19c9>, 2022.
- SNO KARST: Time series of type chemistry in Fontaine de Vaucluse basin, FONTAINE DE VAUCLUSE observatory, KARST observatory network, OZCAR Critical Zone network Research Infrastructure, OSU OREME, [data set], <https://doi.org/10.15148/7b94438a-7bb2-4382-bb25-a4a0c3fdc5d7>, 2021.
- Sorensen, J. P. R., Carr, A. F., Nayebar, J., Diongue, D. M. L., Pouye, A., Roffo, R., Gwengweya, G., Ward, J. S. T., Kanoti, J., Okotto-Okotto, J., van der Marel, L., Ciric, L., Faye, S. C., Gaye, C. B., Goodall, T., Kulabako, R., Lapworth, D. J., MacDonald, A. M., Monjerezi, M., Olago, D., Owor, M., Read, D. S., and Taylor, R. G.: Tryptophan-like and humic-like fluorophores are extracellular in groundwater: implications as real-time faecal indicators, *Sci. Rep.*, 10, 15379, <https://doi.org/10.1038/s41598-020-72258-2>, 2020.
- Stevanović, Z.: Karst waters in potable water supply: a global scale overview, *Environ. Earth Sci.*, 78, 662, <https://doi.org/10.1007/s12665-019-8670-9>, 2019.
- Tucker, S. A., Amszi, V. L., and Acree, W. E.: Primary and secondary inner filtering. Effect of $K_2Cr_2O_7$ on fluorescence emission intensities of quinine sulfate, *J. Chem. Educ.*, 69, <https://doi.org/10.1021/ed069pA8>, 1992.
- White, W. B.: Karst hydrology: recent developments and open questions, *Eng. Geol.*, 65, 85–105, [https://doi.org/10.1016/S0013-7952\(01\)00116-8](https://doi.org/10.1016/S0013-7952(01)00116-8), 2002.
- Zhang, Z., Chen, X., Li, S., Yue, F., Cheng, Q., Peng, T., and Soulsby, C.: Linking nitrate dynamics to water age in underground conduit flows in a karst catchment, *J. Hydrol.*, 596, 125699, <https://doi.org/10.1016/j.jhydrol.2020.125699>, 2021.
- Zsolnay, A., Baigar, E., Jimenez, M., Steinweg, B., and Sacco-mandi, F.: Differentiating with fluorescence spectroscopy the sources of dissolved organic matter in soils subjected to drying, *Chemosphere*, 38, 45–50, [https://doi.org/10.1016/S0045-6535\(98\)00166-0](https://doi.org/10.1016/S0045-6535(98)00166-0), 1999.